scientific reports

OPEN

AKT activation triggers Rab14-mediated ADAM10 translocation to the cell surface in human aortic endothelial cells

Chung Hee Baek[1,4], Hyosang Kim[1,4], Soo Young Moon[2], Eun Kyoung Lee[3] & Won Seok Yang[1]✉

AKT (protein kinase B) activation reduces the harmful effects of advanced glycation end products (AGEs); however, the protective mechanisms remain unknown. In cultured human aortic endothelial cells (HAECs), we investigated how AKT signaling suppresses AGEs-induced intercellular adhesion molecule-1 (ICAM-1) expression. AGEs of bovine serum albumin (AGE-BSA) increased ICAM-1 expression, but this effect was abolished by pretreatment with the AKT activator SC79. SC79 activated AKT1, AKT2, and AKT3, translocated a disintegrin and metalloprotease 10 (ADAM10) to the cell surface, and induced ectodomain shedding of the receptor for AGEs (RAGE). In contrast, GI 254023X-mediated ADAM10 inhibition and siRNA-mediated ADAM10 knockdown both prevented SC79-induced RAGE ectodomain shedding. On the other hand, MK-2206, a pan-AKT inhibitor, and siRNA-mediated knockdown of AKT1, AKT2, or AKT3 prevented SC79-induced ADAM10 cell surface translocation and RAGE ectodomain shedding. Notably, Rab14 was co-immunoprecipitated with ADAM10. Following SC79 treatment, Rab14 moved to the cell surface, whereas siRNA-mediated Rab14 knockdown prevented SC79 from promoting ADAM10 cell surface translocation and RAGE ectodomain shedding and abolished SC79's ability to inhibit AGE-BSA-induced ICAM-1 expression. In conclusion, upon activation of all three isoforms, AKT suppresses AGE-BSA-induced ICAM-1 expression by inducing ADAM10-mediated RAGE ectodomain shedding. This occurs because AKT signaling boosts Rab14-dependent ADAM10 cell surface translocation.

Keywords A disintegrin and metalloprotease 10, AKT, Ectodomain shedding, Receptor for advanced glycation end products, Rab14, SC79

The nonenzymatic glycation and oxidation of proteins, lipids, and nucleic acids produces advanced glycation end products (AGEs)[1]. AGEs bind to the receptor for AGEs (RAGE) on the cell surface, causing inflammatory reactions and contributing to the development of a number of diseases, including atherosclerosis[1]. In contrast, AKT (also known as protein kinase B) activated by insulin-like growth factor-1[2–4] or β-carotene[5] has been shown to alleviate the deleterious effects of AGEs, but the underlying mechanisms are not clear.

RAGE is composed of an extracellular ligand-binding domain, a transmembrane region, and a short cytoplasmic tail[1]. A disintegrin and metalloproteases 10 (ADAM10) cleaves RAGE's extracellular domain near the cell surface[6]. It is synthesized as a pro-ADAM10 in the endoplasmic reticulum (ER) and converted to mature ADAM10 by furin or proprotein convertases in the Golgi apparatus[7,8]. ADAM10 is mostly found in the ER-Golgi apparatus. Upon stimulation, such as through the influx of extracellular Ca^{2+}, ADAM10 promptly translocates to the cell surface and cleaves the extracellular domain of its substrates[9]. However, the translocation process is not yet fully understood. Previously, we found that activating adenosine monophosphate-activated protein kinase (AMPK), either via extracellular Ca^{2+} influx or 5-aminoimidazole-4-carboxamide ribonucleoside (AICAR), causes rapid ADAM10 cell surface translocation in cultured human aortic endothelial cells (HAECs),

[1]Division of Nephrology, Department of Internal Medicine, Asan Medical Center, University of Ulsan College of Medicine, 88 Olympic-ro 43-gil, Songpa-gu, Seoul 05505, Republic of Korea. [2]Asan Institute for Life Sciences, Seoul, Republic of Korea. [3]Division of Nephrology, Department of Internal Medicine, Dankook University Hospital, Dankook University College of Medicine, Cheonan, Republic of Korea. [4]Chung Hee Baek and Hyosang Kim contributed equally as co-first authors. ✉email: wsyang@amc.seoul.kr

which increases ADAM10 shedding activity[10,11]. Importantly, Rab14 was required for AMPK-induced ADAM10 cell surface translocation[11].

Rab14 is one of the Rab GTPases that, when activated, promote the intracellular trafficking of vesicles carrying cargo proteins[12]. In the resting state, TBC1D1 and TBC1D4 suppress Rab14 activation[13]. AMPK and AKT are upstream kinases that phosphorylate TBC1D1 and TBC1D4 at specific residues[14]. Phosphorylated TBC1D1 and TBC1D4 lose their inhibitory action on Rab14[15]. Therefore, activation of AMPK and AKT causes Rab14 to become active.

AKT is a serine/threonine protein kinase that has a pleckstrin homology (PH) domain[16]. To be activated, the PH domain needs to bind PtdIns(3,4,5)P3 on the plasma membrane, which makes the conformation of AKT more amenable to phosphorylation by upstream protein kinases, and the amount of PtdIns(3,4,5)P3 on the plasma membrane determines AKT activation[16]. AKT is composed of AKT1, AKT2, and AKT3 isoforms, each with a specific function. AKT2 is the main AKT isoform that phosphorylates TBC1D1 and TBC1D4 in adipocytes and muscle cells[14,17,18], but all three AKT isoforms contribute to TBC1D4 phosphorylation in neuronal cells[19].

SC79 is a cell-permeable AKT activator. It mimics the action of PtdIns(3,4,5)P3 and binds directly to the PH domain of AKT, activating it[16]. Thereby, SC79 increases the phosphorylation of all three AKT isoforms[16].

Intercellular adhesion molecule-1 (ICAM-1), upregulated by AGEs, promotes inflammatory responses. To find out how AKT signaling lowers the effects of AGEs, we first examined whether activating AKT with SC79 reduces the stimulatory effect of AGEs of bovine serum albumin (AGE-BSA) on ICAM-1 expression. Second, we investigated the possibility that AKT activation promotes ADAM10 cell surface translocation and causes RAGE ectodomain shedding. Third, we looked at the AKT isoforms that are involved in this process. Finally, we investigated the possibility that Rab14 is involved in AKT-induced ADAM10 cell surface translocation.

Results

SC79 reduces AGE-BSA's stimulating effect on ICAM-1 expression

First, we tested whether SC79 pretreatment reduces the stimulating effect of AGE-BSA on ICAM-1 expression. As shown in Fig. 1, AGE-BSA increased ICAM-1 expression, while SC79 pretreatment reduced this effect in a concentration-dependent manner.

SC79 induces the shedding of the RAGE ectodomain

AGE-BSA stimulates ICAM-1 expression via RAGE[10]. We next investigated whether SC79 treatment causes RAGE ectodomain shedding. To see if SC79 induces the release of N-terminal fragments of RAGE, the cells were treated with SC79, and RAGEs in the cell lysate and culture supernatant were quantified by Western blotting with the use of a monoclonal antibody directed against the extracellular domain of human RAGE. As shown in Fig. 2A, SC79 treatment decreased cellular RAGE in a time-dependent manner. In contrast, SC79 treatment raised RAGE levels in the culture supernatant. At doses ranging from 0.1 to 10 μM, SC79 dose-dependently decreased cellular RAGE and increased RAGE in the culture supernatant (Fig. 2B). RAGE in the culture supernatant was somewhat smaller than RAGE in the cell lysates, indicating that it was not full-length RAGE (Fig. 2C).

The increase in RAGE in the culture supernatant can be due to the ectodomain shedding of membrane-bound RAGE or the release of endogenous secretory RAGE (esRAGE), which is produced by alternative mRNA splicing. Ectodomain cleavage of RAGE yields N-terminal and C-terminal fragments, whereas esRAGE does not contain the transmembrane region and the cytosolic tail. To differentiate between the two forms, we examined how SC79 affected the level of the C-terminal fragment of RAGE. As shown in Fig. 2D, treatment with SC79 increased the amount of the C-terminal fragment of RAGE in a dose-dependent manner.

Taken together, the findings that SC79 decreased full-length RAGE in cell lysates while increasing both the N-terminal and C-terminal fragments of RAGE in the culture supernatant and the cell lysates, respectively, indicate that SC79 induces RAGE ectodomain shedding. The N-terminal fragment of RAGE in the culture supernatant (Fig. 2A and B) and the C-terminal fragment of RAGE in the cell lysates (Fig. 2D) were also visible in the control condition, indicating that cells shed RAGE constitutively.

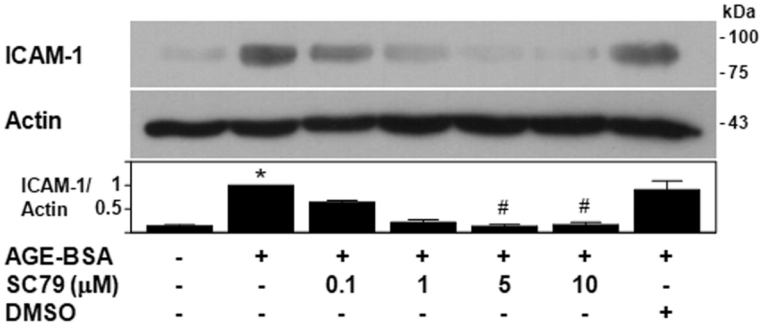

Fig. 1. SC79 reduces AGE-BSA's stimulating effect on ICAM-1 expression. HAECs were pre-incubated with different concentrations of SC79 for 30 min, and then they were co-incubated with AGE-BSA (100 μg/ml) for 24 h. The cell lysates were immunoblotted with antibodies against ICAM-1 and actin. ($n = 3$, $^{*}p < 0.05$ vs. control; $^{\#}p < 0.05$ vs. AGE-BSA)

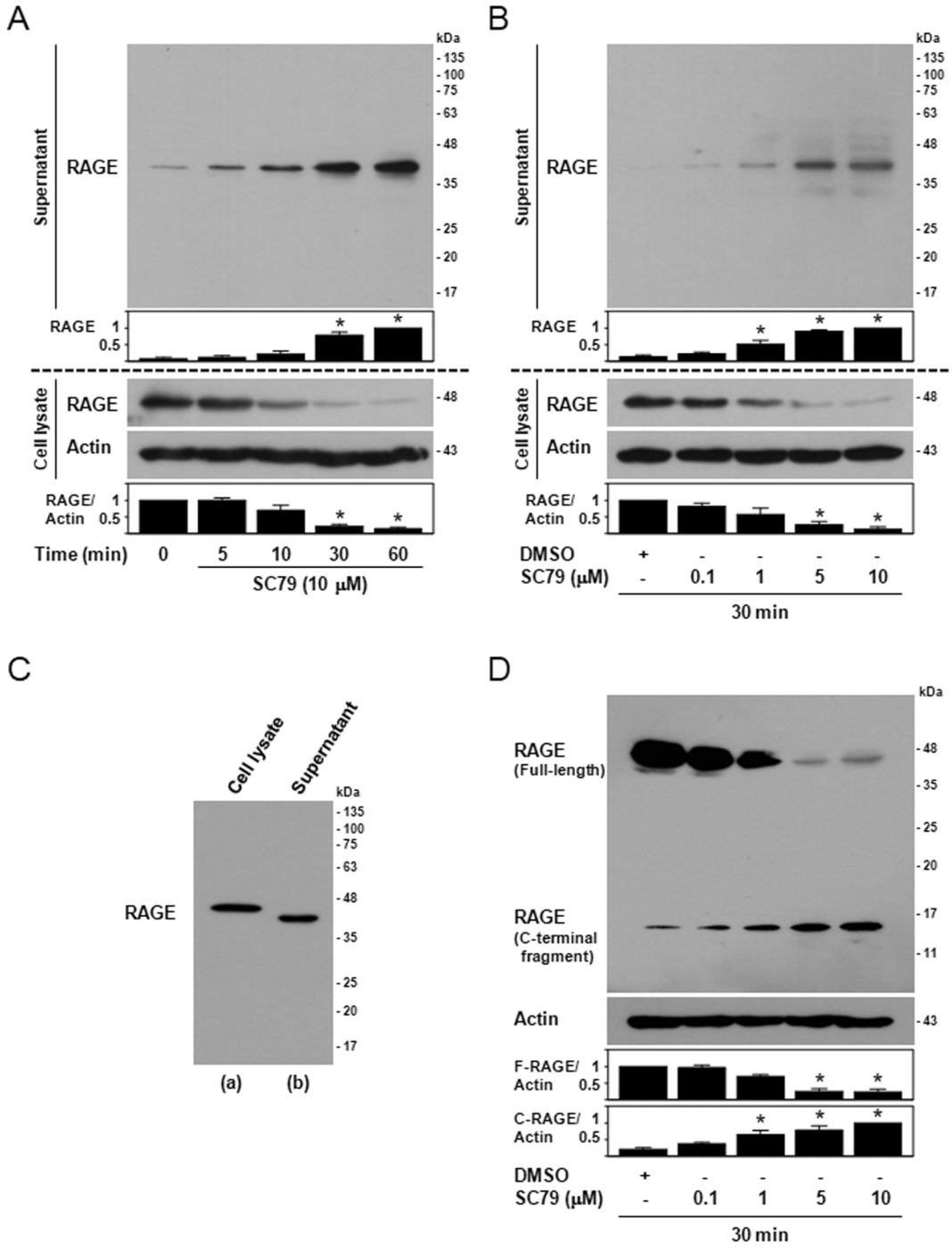

Fig. 2. SC79 induces the shedding of the RAGE ectodomain. HAECs were incubated with 10 μM SC79 for various times (5, 10, 30, and 60 min) ($n = 4$) (**A**) or different concentrations of SC79 (0.1, 1, 5, and 10 μM) for 30 min ($n = 3$) (**B**). The cell lysate and culture supernatant were immunoblotted with a monoclonal antibody to the extracellular domain of human RAGE and an anti-actin antibody. To compare the size of RAGE in cell lysate and culture supernatant, untreated cell lysate (a) and conditioned media from cells treated with 10 μM SC79 for 30 min (b) were run on the same gel and immunoblotted with the RAGE antibody (**C**). The cell lysates of HAECs treated with different concentrations of SC79 (0.1, 1, 5, and 10 μM) for 30 min were immunoblotted with an antibody to the C-terminal domain of human RAGE and an anti-actin antibody (n = 4) (**D**). ($^{*}p < 0.05$ vs. control)

Inhibitors of AKT and ADAM10 diminish SC79-induced RAGE ectodomain shedding

SC79 is a pan-AKT activator. ADAM10, ADAM17, and matrix metalloproteinase 9 are all known to cleave RAGE in the ectodomain[20,21]. According to the literature, AKT was expected to increase ADAM10 activity. Thus, we explored whether AKT and ADAM10 are involved in SC79-induced RAGE ectodomain shedding. MK-2206,

a pan-AKT inhibitor, and GI 254023X, an ADAM10 inhibitor, both prevented SC79-induced increases in the N-terminal fragment of RAGE in the culture supernatant (Fig. 3). The almost complete inhibition seen with GI 254023X provides more evidence that enzymatic cleavage, not the release of a spliced form of RAGE, is the mechanism.

SC79-induced RAGE ectodomain shedding is mediated by AKT1/2/3 activation

HAECs expressed all three AKT isoforms, including AKT1, AKT2, and AKT3 (Fig. 4A). We investigated which AKT isoforms are involved in SC79-induced RAGE ectodomain shedding. AKT is activated by phosphorylations at threonine 308/309/305 and serine 473/474/472 in AKT1/AKT2/AKT3, respectively[22]. To ascertain activation, we assessed the phosphorylations of AKT1 Ser473, AKT2 Ser474, and AKT3 Ser472. To deplete each AKT isoform, siRNAs were transfected, and we verified that AKT1-, AKT2-, and AKT3-siRNAs significantly reduced each AKT isoform specifically (Fig. 4A).

SC79 increased AKT1, AKT2, and AKT3 phosphorylations (Fig. 4B, 5A, 6A). In contrast, siRNA-mediated knockdown of AKT1, AKT2, or AKT3 prevented SC79-induced RAGE ectodomain shedding (Fig. 4C, 5B, 6B).

We then investigated the possibility that AKT1, AKT2, and AKT3 mediate SC79's suppression of the stimulatory effect of AGE-BSA on ICAM-1 expression. As shown in Fig. 4D, 5C, and 6C, the depletion of AKT1, AKT2, or AKT3 by siRNA abrogated SC79's inhibitory effect on AGE-BSA-induced ICAM-1 expression.

The results indicate that AKT1, AKT2, and AKT3 are all required for SC79-induced RAGE ectodomain shedding.

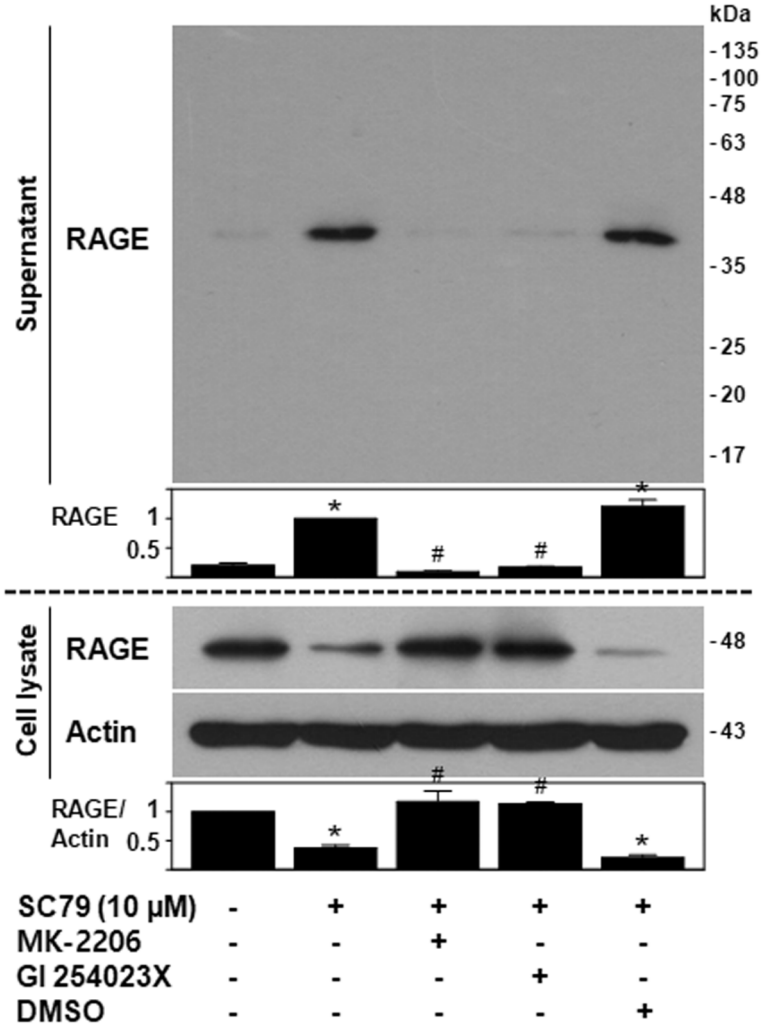

Fig. 3. Inhibitors of AKT and ADAM10 diminish SC79-induced RAGE ectodomain shedding. HAECs were preincubated with or without MK-2206 (1 μM), GI 254023X (2 μM), or DMSO (vehicle) for 60 min. Following this, they were further incubated for 30 min with or without SC79 (10 μM). The cell lysate and culture supernatant were immunoblotted with a monoclonal antibody to the extracellular domain of human RAGE and an anti-actin antibody. ($n = 3$, $^{*}p < 0.05$ vs. control, $^{\#}p < 0.05$ vs. SC79 treatment alone)

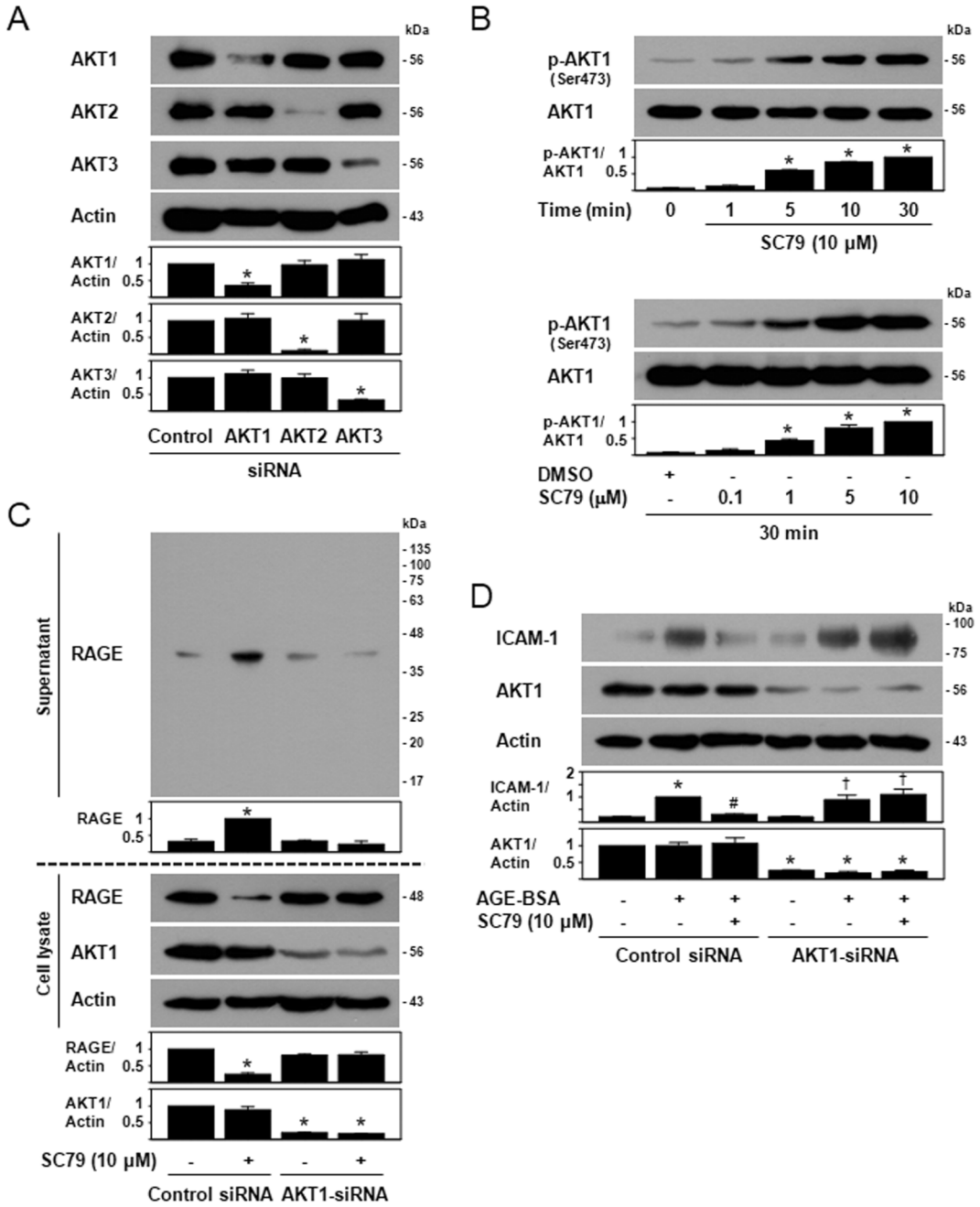

Fig. 4. AKT1 activation is required for SC79-induced RAGE ectodomain shedding. (**A**) HAECs express all three AKT isoforms, and AKT1-, AKT2-, and AKT3-siRNAs selectively deplete each AKT isoform. HAECs were transfected with AKT1-, AKT2-, AKT3-siRNAs, or control siRNAs, and the cell lysates were immunoblotted with antibodies to AKT1, AKT2, AKT3, or actin. ($n = 3$, $^{*}p < 0.05$ vs. control). (**B**) SC79 activates AKT1. HAECs were incubated with 10 μM SC79 for various times (1, 5, 10, and 30 min) (upper panel) or different concentrations of SC79 (0.1, 1, 5, and 10 μM) for 30 min (lower panel). The cell lysates were immunoblotted with antibodies to p-AKT1 (Ser473) and AKT1. ($n = 3$, $^{*}p < 0.05$ vs. control). (**C**) AKT1 knockdown inhibits SC79-induced RAGE ectodomain shedding. HAECs were transfected with AKT1-siRNA or control siRNA and then incubated for 30 min with or without SC79 (10 μM). The cell lysate and culture supernatant were immunoblotted with a monoclonal antibody to the extracellular domain of human RAGE and antibodies to AKT1 and actin. ($n = 3$, $^{*}p < 0.05$ vs. control cells transfected with control siRNA). (**D**) AKT1 knockdown abolishes SC79's inhibitory effect against AGE-BSA. HAECs transfected with AKT1-siRNA or control siRNA were treated for 30 min with or without SC79 (10 μM). The cells were then treated with AGE-BSA (100 μg/ml) for 24 h. The cell lysates were immunoblotted with antibodies to ICAM-1, AKT1, and actin. ($n = 3$, $^{*}p < 0.05$ vs. control; $^{\#}p < 0.05$ vs. AGE-BSA; $^{\dagger}p < 0.05$ vs. control cells transfected with AKT1-siRNA)

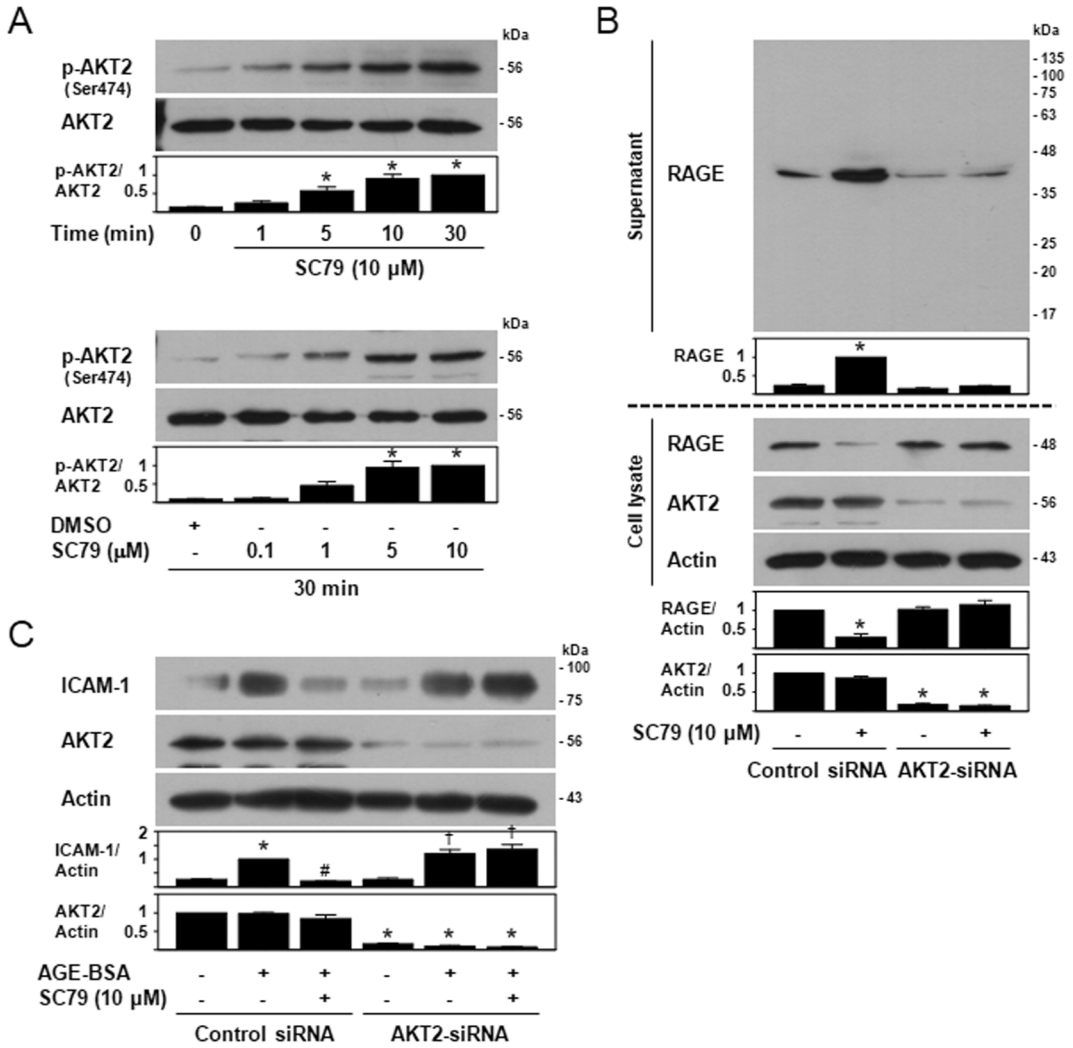

Fig. 5. AKT2 activation is required for SC79-induced RAGE ectodomain shedding. (**A**) SC79 activates AKT2. HAECs were incubated with 10 μM SC79 for various times (1, 5, 10, and 30 min) (upper panel) or different concentrations of SC79 (0.1, 1, 5, and 10 μM) for 30 min (lower panel). The cell lysates were immunoblotted with antibodies to p-AKT2 (Ser474) and AKT2. ($n = 4$, $^{*}p < 0.05$ vs. control). (**B**) AKT2 knockdown inhibits SC79-induced RAGE ectodomain shedding. HAECs were transfected with AKT2-siRNA or control siRNA and then incubated for 30 min with or without SC79 (10 μM). The cell lysate and culture supernatant were immunoblotted with a monoclonal antibody to the extracellular domain of human RAGE and antibodies to AKT2 and actin. ($n = 4$, $^{*}p < 0.05$ vs. control cells transfected with control siRNA). (**C**) AKT2 knockdown abolishes SC79's inhibitory effect against AGE-BSA. HAECs transfected with AKT2-siRNA or control siRNA were treated for 30 min with or without SC79 (10 μM). The cells were then treated with AGE-BSA (100 μg/ml) for 24 h. The cell lysates were immunoblotted with antibodies to ICAM-1, AKT2, and actin. ($n = 3$, $^{*}p < 0.05$ vs. control; $^{\#}p < 0.05$ vs. AGE-BSA; $^{\dagger}p < 0.05$ vs. control cells transfected with AKT2-siRNA)

SC79 induces RAGE ectodomain shedding by promoting ADAM10 cell surface translocation

We examined the cell surface expression of ADAM10 before and after SC79 treatment by immunofluorescently labeling nonpermeabilized cells with an antibody against an extracellular epitope of the protein. In untreated cells, ADAM10 was weakly positive on the cell surface. However, following 20 and 30 min of SC79 treatment, there was a considerable rise in cell surface ADAM10 (Fig. 7A). The cell surface ADAM10 returned to near baseline at 60 min. We also evaluated the quantity of ADAM10 protein in the cell lysates from the cells in the same culture dish but not utilized for immunofluorescent staining. There was no appreciable change in the amount of cellular ADAM10 protein following SC79 treatment (Fig. 7A). The findings suggest that SC79 translocates ADAM10 to the cell surface from intracellular compartments.

Next, we used siRNA-mediated ADAM10 depletion to examine the impact of selective ADAM10 inhibition on SC79-induced RAGE ectodomain shedding. ADAM10-siRNA significantly reduced ADAM10 and prevented SC79-induced RAGE ectodomain shedding, as shown in Fig. 7B. On the other hand, the constitutive shedding of RAGE appeared to be insensitive to the reduction of ADAM10. This may be because other matrix metalloproteinases, including ADAM17[21], also participate in RAGE ectodomain shedding.

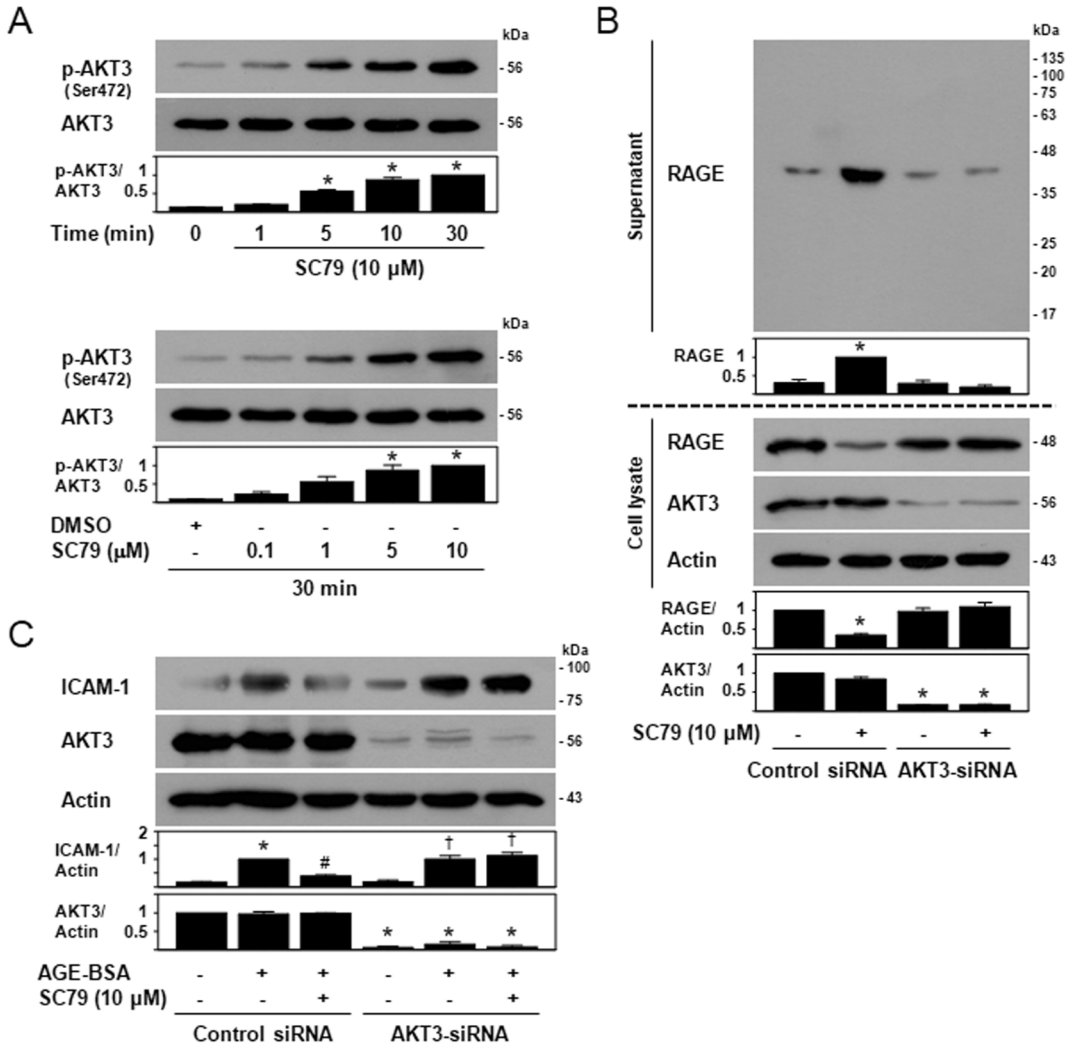

Fig. 6. AKT3 activation is required for SC79-induced RAGE ectodomain shedding. (**A**) SC79 activates AKT3. HAECs were incubated with 10 μM SC79 for various times (1, 5, 10, and 30 min) (upper panel) or different concentrations of SC79 (0.1, 1, 5, and 10 μM) for 30 min (lower panel). The cell lysates were immunoblotted with antibodies to p-AKT3 (Ser472) and AKT3. ($n = 3$, $^{*}p < 0.05$ vs. control). (**B**) AKT3 knockdown inhibits SC79-induced RAGE ectodomain shedding. HAECs were transfected with AKT3-siRNA or control siRNA and then incubated for 30 min with or without SC79 (10 μM). The cell lysate and culture supernatant were immunoblotted with a monoclonal antibody to the extracellular domain of human RAGE and antibodies to AKT3 and actin. ($n = 3$, $^{*}p < 0.05$ vs. control cells transfected with control siRNA). (**C**) AKT3 knockdown abolishes SC79's inhibitory effect against AGE-BSA. HAECs transfected with AKT3-siRNA or control siRNA were treated for 30 min with or without SC79 (10 μM). The cells were then treated with AGE-BSA (100 μg/ml) for 24 h. The cell lysates were immunoblotted with antibodies to ICAM-1, AKT3, and actin. ($n = 3$, $^{*}p < 0.05$ vs. control; $^{\#}p < 0.05$ vs. AGE-BSA; $^{\dagger}p < 0.05$ vs. control cells transfected with AKT3-siRNA)

In line with its effect on RAGE ectodomain shedding, siRNA-mediated ADAM10 depletion abolished SC79's inhibitory effect on AGE-BSA-induced ICAM-1 expression (Fig. 7C).

Depletion of AKT1, AKT2, or AKT3 impairs SC79-induced ADAM10 cell surface translocation

We further examined the role of AKT activation in SC79-induced ADAM10 cell surface translocation. MK-2206, a pan-AKT inhibitor, blocked the SC79-induced increase in ADAM10 expression on the cell surface (Fig. 8A). We transfected siRNAs to identify the AKT isoforms involved. As shown in Fig. 8B, C, and D, siRNA-mediated reductions of AKT1, AKT2, and AKT3 inhibited SC79-induced increases in ADAM10 expression on the cell surface. The results indicate that AKT1, AKT2, and AKT3 are all required for SC79-induced ADAM10 cell surface translocation.

Rab14 interacts with ADAM10 and, upon SC79 treatment, moves to the cell surface

Rab14, a small GTPase, is involved in the translocation of ADAM10 to the cell surface after AMPK activation[11]. Like AMPK, AKT activates Rab14. In general, the Rab attached to a specific type of vesicle emanating from

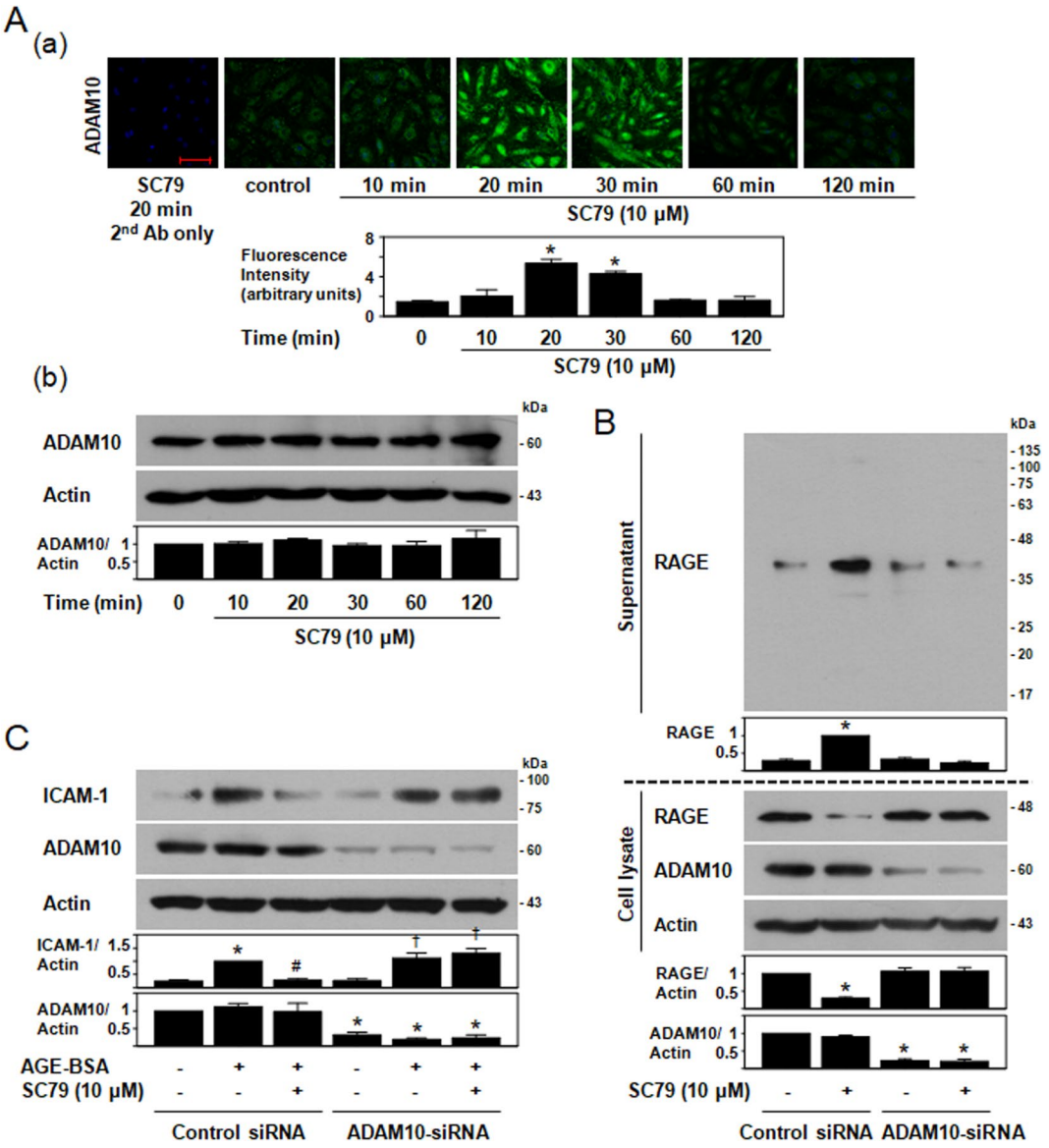

Fig. 7. SC79 induces RAGE ectodomain shedding by promoting ADAM10 cell surface translocation. (**A**) Immunofluorescence staining to evaluate the effect of SC79 on ADAM10 localization. HAECs grown in culture dishes with a coverslip were treated with SC79 (10 μM) for 10–120 min. (a) The cells on the coverslip were fixed for 10 min with 4% paraformaldehyde without permeabilization, then immunostained with an antibody to an extracellular portion of ADAM10 and examined using confocal microscopy. DAPI was used to label the nuclei of the cells. Representative photos and the relative fluorescence intensities are shown (scale bar: 100 μm). (b) Cell lysates from cells that were not on the coverslip in the same culture plate were immunoblotted with antibodies to ADAM10 and actin. ($n = 3$, $^{*}p < 0.05$ vs. control). (**B**) ADAM10 knockdown inhibits SC79-induced RAGE ectodomain shedding. HAECs were transfected with ADAM10-siRNA or control siRNA and then incubated for 30 min with or without SC79 (10 μM). The cell lysate and culture supernatant were immunoblotted with a monoclonal antibody to the extracellular domain of human RAGE and antibodies to ADAM10 and actin. ($n = 3$, $^{*}p < 0.05$ vs. control cells transfected with control siRNA). (**C**) ADAM10 knockdown abolishes SC79's inhibitory effect against AGE-BSA. HAECs transfected with ADAM10-siRNA or control siRNA were treated for 30 min with or without SC79 (10 μM). The cells were then treated with AGE-BSA (100 μg/ml) for 24 h. The cell lysates were immunoblotted with antibodies to ICAM-1, ADAM10, and actin. ($n = 3$, $^{*}p < 0.05$ vs. control; $^{\#}p < 0.05$ vs. AGE-BSA; $^{\dagger}p < 0.05$ vs. control cells transfected with ADAM10-siRNA)

the donor membrane is activated by GDP-GTP conversion and facilitates vesicle transport. During vesicle trafficking, the Rab also reaches the target membrane[23,24] and aids in the vesicle's membrane fusion. Thus, we explored whether Rab14 interacts with ADAM10 and whether Rab14 also moves to the cell surface after SC79 treatment.

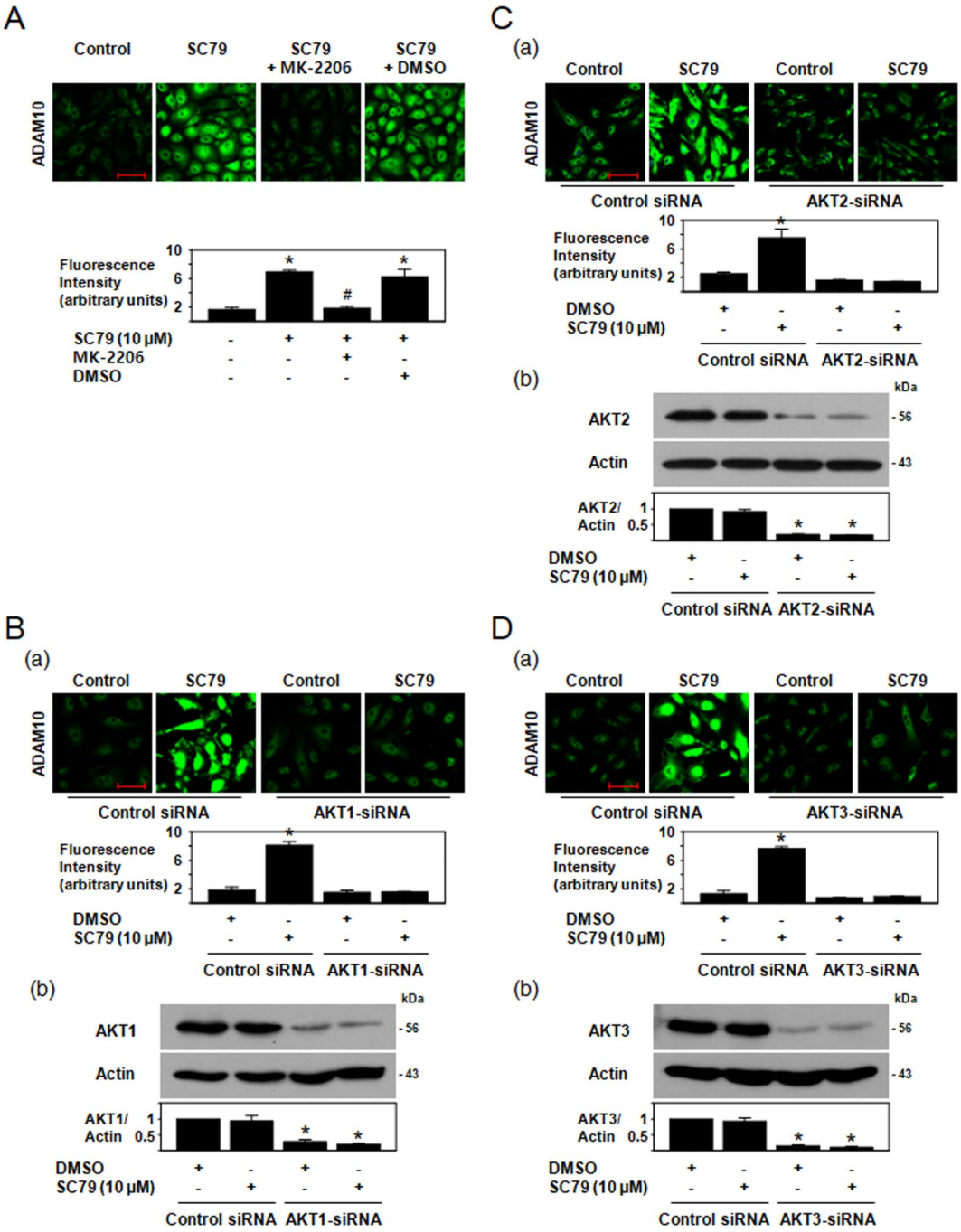

Fig. 8. Depletion of AKT1, AKT2, or AKT3 impairs SC79-induced ADAM10 cell surface translocation. (**A**) AKT inhibition prevents SC79-induced ADAM10 cell surface translocation. HAECs were preincubated with or without MK-2206 (1 μM) or DMSO (vehicle) for 60 min. Following this, they were further incubated for 20 min with or without SC79 (10 μM). Cells were immunostained with an antibody to an extracellular portion of ADAM10. Representative photos and the relative fluorescence intensities are shown (scale bar: 100 μm). ($n = 3$, $^{*}p < 0.05$ vs. control; $^{\#}p < 0.05$ vs. SC79 treatment alone). (**B**–**D**) AKT1, AKT2, and AKT3 knockdowns prevent SC79-induced ADAM10 cell surface translocation. HAECs grown in culture dishes with a coverslip were transfected with AKT1-siRNA, AKT2-siRNA, AKT3-siRNA, or control siRNA, and then incubated for 20 min with DMSO or SC79 (10 μM). (a) Cells grown on the coverslip were immunostained for ADAM10. Representative photos and the relative fluorescence intensities are shown (scale bar: 100 μm). (b) Cell lysates from cells that were not on the coverslip in the same culture plate were immunoblotted with antibodies to AKT1, AKT2, AKT3, or actin. ($n = 3$, $^{*}p < 0.05$ vs. control cells transfected with control siRNA)

We used co-immunoprecipitation to investigate the possible interaction between Rab14 and ADAM10. In the basal state, Rab14 was specifically co-immunoprecipitated with ADAM10 (Fig. 9A). The amount of co-immunoprecipitated Rab14 slightly increased after 20 min of SC79 treatment, but this increase was not statistically significant when adjusted for ADAM10.

To further study SC79's effect on ADAM10 and Rab14 localization, we labeled cell surface proteins with biotin, separated cell surface and intracellular proteins with avidin-coated agarose beads, and quantified ADAM10 and Rab14 in each sample by Western blotting. As shown in Fig. 9B, SC79 increased cell surface ADAM10 while decreasing intracellular ADAM10, confirming the results of ADAM10 immunofluorescent staining. Likewise, SC79 increased biotin-captured Rab14 while decreasing intracellular Rab14. On the other hand, overall levels of ADAM10 and Rab14 were unaffected by SC79 treatment for 20 min.

The findings indicate that both ADAM10 and Rab14 move to the cell surface following SC79 treatment.

Rab14 is required for SC79-induced ADAM10 cell surface translocation

Next, we investigated whether Rab14 is necessary for the cell surface translocation of ADAM10 caused by SC79 and the subsequent ectodomain shedding of RAGE.

Transfection of Rab14-siRNA markedly reduced Rab14 protein and prevented SC79-induced ADAM10 cell surface translocation (Fig. 10A) and RAGE ectodomain shedding (Fig. 10B), which indicates that Rab14 is essential for SC79-induced ADAM10 cell surface translocation.

Finally, we examined whether Rab14 is involved in SC79's inhibitory effect on AGEs. As shown in Fig. 10C, the knockdown of Rab14 with siRNA eliminated SC79's inhibitory effect on AGE-BSA-induced ICAM-1 expression.

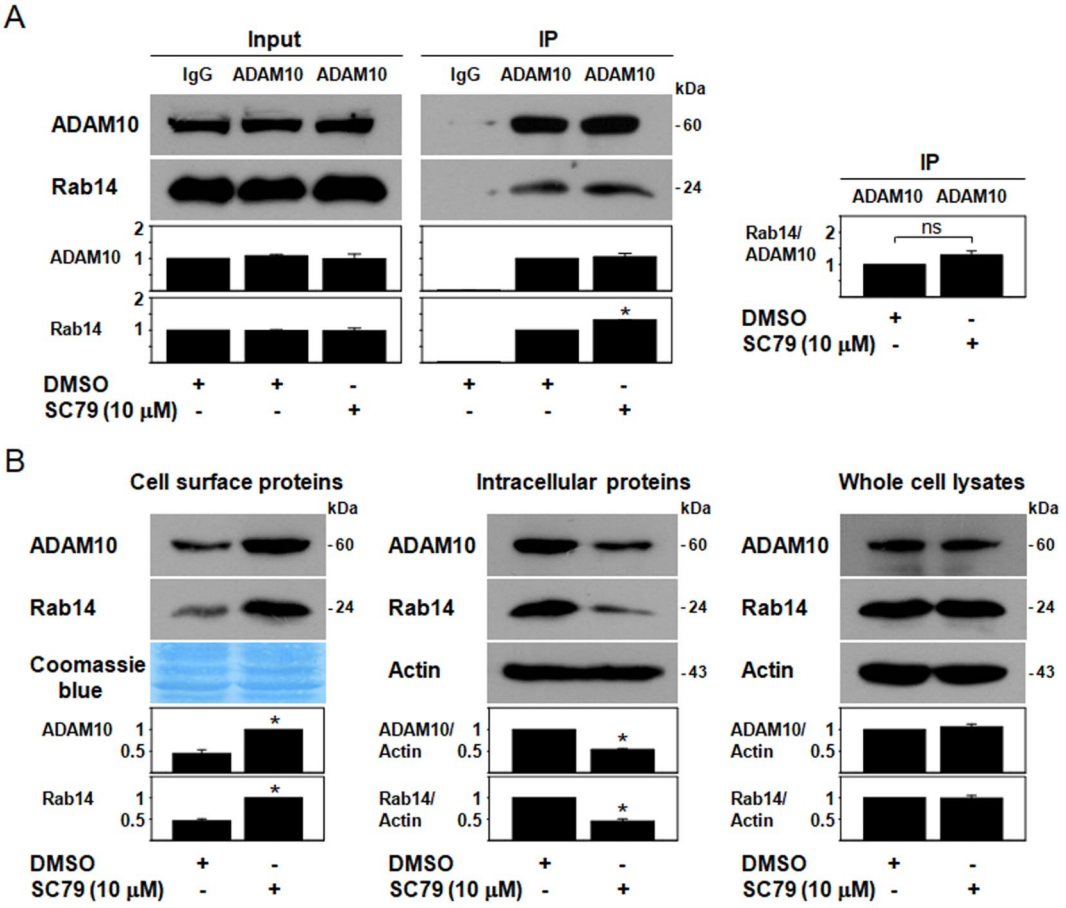

Fig. 9. Rab14 interacts with ADAM10 and, upon SC79 treatment, moves to the cell surface. (**A**) Rab14 co-immunoprecipitates with ADAM10. HAECs were treated with DMSO or SC79 (10 μM) for 20 min before being lysed with NP-40 buffer. Lysates were incubated with rabbit anti-ADAM10 antibody or rabbit IgG as a control overnight at 4 °C, followed by incubation with Protein A agarose. The input and immunoprecipitation fractions were analyzed using anti-ADAM10 and anti-Rab14 antibodies. ($n = 4$, $^{*}p < 0.05$ vs. cells treated with DMSO and immunoprecipitated with ADAM10 antibody, ns: not significant). (**B**) SC79 translocates ADAM10 and Rab14 from intracellular compartments to the cell surface. HAECs were treated with DMSO or SC79 (10 μM) for 20 min. The cell surface proteins were biotin-labeled and isolated with avidin-coated agarose beads. Whole cell lysates, biotin-bound cell surface proteins, and biotin-unbound intracellular proteins were examined by Western blotting using anti-ADAM10, Anti-Rab14, and anti-actin antibodies. ($n = 5$, $^{*}p < 0.05$)

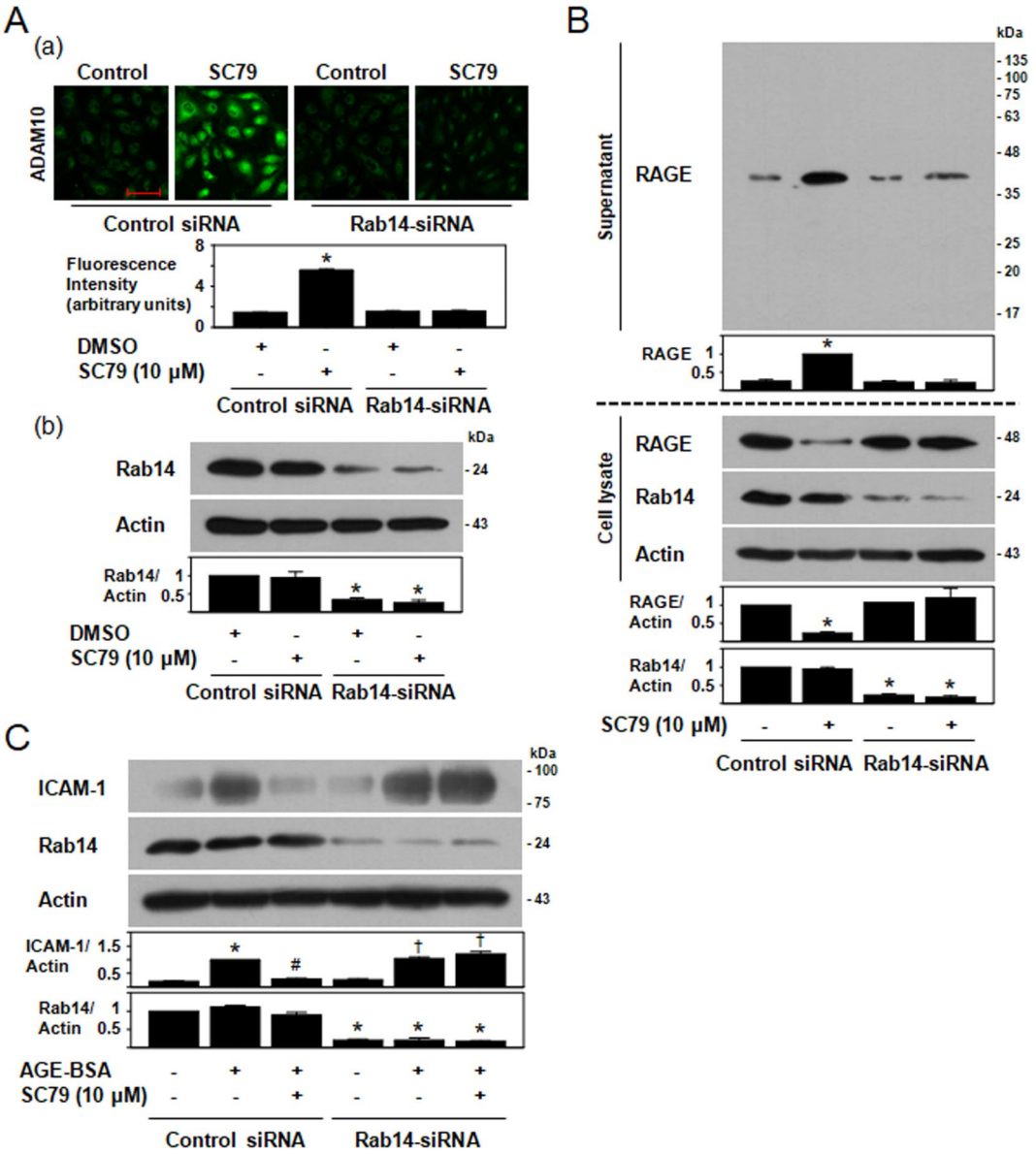

Fig. 10. Rab14 is required for SC79-induced ADAM10 cell surface translocation. (**A**) Rab14 knockdown prevents SC79-induced ADAM10 cell surface translocation. HAECs grown in culture dishes with a coverslip were transfected with Rab14-siRNA or control siRNA and then incubated for 20 min with DMSO or SC79 (10 μM). (a) Cells grown on the coverslip were immunostained with an antibody to an extracellular portion of ADAM10. Representative photos and the relative fluorescence intensities are shown (scale bar: 100 μm). (b) Cell lysates from cells that were not on the coverslip in the same culture plate were immunoblotted with antibodies to Rab14 and actin. ($n = 3$, $^{*}p < 0.05$ vs. control cells transfected with control siRNA). (**B**) Rab14 knockdown inhibits SC79-induced RAGE ectodomain shedding. HAECs were transfected with Rab14-siRNA or control siRNA and then incubated for 30 min with or without SC79 (10 μM). The cell lysate and culture supernatant were immunoblotted with a monoclonal antibody to the extracellular domain of human RAGE and antibodies to Rab14 and actin. ($n = 3$, $^{*}p < 0.05$ vs. control cells transfected with control siRNA). (**C**) Rab14 knockdown abolishes SC79's inhibitory effect against AGE-BSA. HAECs transfected with Rab14-siRNA or control siRNA were treated for 30 min with or without SC79 (10 μM). The cells were then treated with AGE-BSA (100 μg/ml) for 24 h. The cell lysates were immunoblotted with antibodies to ICAM-1, Rab14, and actin. ($n = 4$, $^{*}p < 0.05$ vs. control; $^{\#}p < 0.05$ vs. AGE-BSA; $^{\dagger}p < 0.05$ vs. control cells transfected with Rab14-siRNA)

Discussion

SC79 attenuated the impact of AGE-BSA, which elevates ICAM-1 expression in HAECs. Our findings show that the inhibition caused by SC79 is driven by AKT activation, which facilitates ADAM10-mediated shedding of the RAGE ectodomain. More importantly, this study reveals that the activation of AKT signaling boosts the Rab14-dependent translocation of ADAM10 to the cell surface, thereby increasing its shedding activity.

In this study, AGE-BSA enhanced the expression of ICAM-1 in HAECs. Pretreatment with SC79, on the other hand, blocked the effect of AGE-BSA. By activating AKT, SC79 induced RAGE ectodomain shedding. SC79's inhibitory effect on AGE-BSA-induced ICAM-1 expression, on the other hand, was reversed by inhibiting RAGE ectodomain shedding. As a result, the protective effect of AKT activation against AGEs was related to RAGE ectodomain shedding. Cleavage of the extracellular domain eliminates cell surface RAGEs, reducing the vulnerability of the cell to AGEs. Moreover, the released extracellular domain of RAGE neutralizes AGEs[25].

ADAM10 was implicated in the cleavage of the RAGE extracellular domain following SC79 treatment because SC79 increased ADAM10 cell surface expression, whereas ADAM10 inhibition by GI 254023X and ADAM10 knockdown by siRNA blocked RAGE ectodomain shedding. The increase in ADAM10 cell surface expression coincided with a decrease in intracellular ADAM10, whereas SC79 had no impact on the overall quantity of ADAM10. Hence, the SC79-induced increase of ADAM10 on the cell surface was caused by its translocation from intracellular compartments to the cell surface rather than new production.

In a previous study[26], AKT was suggested to play a role in the activation of ADAM10. Klotho is a transmembrane protein that has anti-aging properties. In Klotho-transfected COS-7 cells, insulin treatment increased ADAM10-mediated ectodomain shedding of Klotho via a phosphoinositide 3-kinase (PI3K)/AKT-dependent mechanism. This occurred despite no increase in ADAM10 mRNA or protein level, implying that insulin works by enhancing ADAM10 shedding activity. However, the underlying mechanism has not been further identified. In the current study, the stimulatory effects of SC79 on ADAM10 cell surface translocation and ADAM10-mediated RAGE ectodomain shedding were abolished by siRNA-mediated reduction of AKT1, AKT2, or AKT3 as well as MK-2206, a pan-AKT inhibitor, indicating that SC79's actions were dependent on AKT. Overall, our findings suggest that AKT activation boosts ADAM10 shedding activity by promoting ADAM10 cell surface translocation.

Notably, Rab14 was required for AKT-induced ADAM10 cell surface translocation. Rab GTPases control the trafficking of cell surface proteins from the Golgi apparatus to the plasma membrane, and about 60 different Rab GTPases have been identified[12]. In muscle cells[27] and adipocytes[28], Rab14 is implicated in the translocation of glucose transporter 4 (GLUT4) to the cell surface, which promotes cellular glucose uptake. Rab14 is also involved in ADAM10 cell surface trafficking, which was first found in the study of wound healing assays using a monolayer of A549 cells[29]. The damage to the cell layer caused the remaining cells to migrate to the empty area; however, Rab14 knockdown prevented this migration. This was because Rab14 is required for ADAM10 translocation to the cell surface to remove N-cadherin, a cell adhesion molecule, which allows cells to migrate to the vacant area. In a previous study[11], we found that activating AMPK promotes ADAM10 cell surface translocation in HAECs, and Rab14 is involved in this process. In the present study, Rab14 was co-immunoprecipitated with ADAM10. Following SC79 treatment, Rab14 moved to the cell surface, whereas siRNA-mediated Rab14 knockdown blocked SC79-induced ADAM10 cell surface translocation and RAGE ectodomain shedding, suggesting that Rab14 is also essential for AKT-induced ADAM10 cell surface translocation.

Rab14 is a downstream component of both the AMPK and AKT signaling pathways. The two signaling pathways have been well established in studies of exercise- and insulin-induced GLUT4 cell surface translocation in muscle cells. Exercise and insulin activate AMPK and AKT, respectively[13]. Rab GTPases are active when coupled to GTP but inactive when linked to GDP. They are activated by guanine nucleotide exchange factors (GEFs), which enhance GTP binding, and deactivated by Rab GTPase-activating proteins (RabGAPs), which promote GTP hydrolysis[13]. FAM116 proteins serve as Rab14 GEFs[29], whereas TBC1D1 and TBC1D4 are RabGAPs that inhibit Rab14 and several other Rab GTPases[13]. On the other hand, TBC1D1 and TBC1D4 are substrates of AMPK and AKT. When TBC1D1 and TBC1D4 are phosphorylated by AMPK or AKT, their inhibitory effects on Rab GTPases are removed, allowing Rab GTPases to be activated[13,15], leading to enhanced GLUT4 cell surface trafficking[13]. As Rab14 is also implicated in ADAM10 cell surface translocation, AMPK or AKT activation is expected to enhance ADAM10 cell surface translocation. Consistent with this notion, our previous[11] and current findings indicate that Rab14-activating signals, such as AMPK and AKT, are the triggers of ADAM10 shedding activity. However, Rab14 is not the only factor necessary for ADAM10 trafficking. Since the literature indicates that the TspanC8 family of tetraspanins regulates ADAM10 trafficking[30], it may be necessary to explore how the tetraspanins participate in ADAM10 translocation to the cell surface induced by AMPK and AKT.

The AKT isoform(s) that control TBC1D1/TBC1D4 varied depending on the type of cell. In adipocytes and muscle cells, AKT2 plays a major role in the phosphorylation of TBC1D1/TBC1D4, which leads to Rab14 activation[18]. In neuronal cells, however, all three AKT isoforms contribute to TBC1D4 phosphorylation[19]. The reasons for these differences are unclear. In this study, SC79 needed AKT1, AKT2, and AKT3 to induce Rab14-dependent ADAM10 cell surface translocation and RAGE ectodomain shedding, which suggests that each isoform has a distinct role.

AGEs elicit inflammatory reactions by activating RAGE signaling[1]. A previous study[31] showed that AGE-BSA activates AKT in HAECs. On the other hand, in this study, AKT activation reduced cell surface RAGE. As a result, it's plausible that AGE-induced AKT activation works as a negative feedback regulator, preventing potentially detrimental inflammatory reactions to prolonged AGE exposure.

There has been evidence that SC79 suppresses the effects of lipopolysaccharide (LPS) and tumor necrosis factor-α (TNF-α) by activating AKT. In microglia, SC79 inhibited LPS-induced NADPH oxidase 2 expression, reactive oxygen species production, and glutamate release[32]. In mice with LPS-induced sepsis, SC79 treatment significantly decreased serum IL-1β and improved survival[33]. PI3K/AKT inhibition, on the other hand, greatly exacerbated LPS-induced inflammation, resulting in lower survival in endotoxemic mice[34]. SC79 was also shown to attenuate TNF-α-induced apoptosis in hepatocytes[35]. In an animal experiment, SC79 protected mice from D-galactosamine/LPS-induced TNF-α-mediated liver injury, whereas LY294002, a PI3K/AKT inhibitor, abrogated SC79's hepatoprotective effects[35]. In this regard, our findings suggest plausible mechanisms for the protective effects of SC79. Toll-like receptor 4 (TLR4) and tumor necrosis factor receptor 1 (TNFR1), which are receptors for LPS and TNF-α, respectively, are ADAM10 substrates. Therefore, it may be possible that AKT

activation induces ADAM10-mediated ectodomain shedding of TLR4 and TNFR1, which results in protective effects against LPS and TNF-α.

In conclusion, upon activation of all three isoforms, AKT suppresses AGE-BSA-induced ICAM-1 expression by inducing ADAM10-mediated RAGE ectodomain shedding. This occurs because AKT signaling boosts Rab14-dependent ADAM10 cell surface translocation.

Materials and methods

Reagents

SC79 (HY-18749) and MK-2206 (HY-10358) were purchased from MedChemExpress (Brea, CA, USA). AGE-BSA was from Cayman Chemical (Ann Arbor, MI, USA). GI 254023X, 4′,6-diamidino-2-phenylindole (DAPI), and dimethyl sulfoxide (DMSO) were from Sigma-Aldrich (St. Louis, MO, USA). SC79, MK-2206, and GI 254023X were dissolved in DMSO. Antibodies for human RAGE (sc-80652; a mouse monoclonal antibody against a truncated extracellular domain of human RAGE), ADAM10 (sc-28358; a mouse monoclonal antibody for Western blotting), Rab14 (sc-271401; a mouse monoclonal antibody), ICAM-1 (sc-7891), and actin (sc-47778) were from Santa Cruz Biotechnology (Dallas, TX, USA). Anti-RAGE (JF0975) rabbit monoclonal antibody against amino acids 350–390 corresponding to the C-terminal region of human RAGE was from R&D Systems, Inc. (Minneapolis, MN, USA). Rabbit polyclonal antibodies against the amino acids 214–500 of human ADAM10 (A10438; for immunofluorescence staining), AKT1 (A11016), AKT3 (A12909), p-AKT1^{Ser473} (AP0140), and p-AKT2^{Ser474} (AP0005) were from ABclonal, Inc. (Woburn, MA, USA). AKT2 antibody (#3063) was from Cell Signaling Technology, Inc. (Danvers, MA, USA). p-AKT3^{Ser472} (PAB8141) antibody was from Abnova Corporation (Taipei, Taiwan). ADAM10 recombinant rabbit monoclonal antibody (JM32-11) (MA5-32616; for immunoprecipitation), ADAM10-small interfering RNA (siRNA), Rab14-siRNA, and control siRNA (Ambion®) were from ThermoFisher Scientific. AKT1-siRNA (sc-29195), AKT2-siRNA (sc-29197), AKT3-siRNA (sc-38911), and the corresponding control siRNA (sc-37007) were from Santa Cruz Biotechnology, Inc.

Cell culture

Primary HAECs were acquired from Lonza Walkersville (Walkersville, MD, USA) and cultivated in EBM-2 endothelial growth basal media (Lonza Walkersville). After 3–5 passages, equal numbers of cells were plated on tissue culture plates and cultured for 24 h before resting for 16 h in Medium 199 with Hank's salts (ThermoFisher Scientific) containing 2% fetal calf serum. The culture medium was then changed to serum-free Medium 199 with Hank's salts (Ca^{2+} 1.26 mM), and the cells were subjected to the experiments.

Transfection with siRNA

Lipofectamine (Life Technologies/ThermoFisher Scientific) was used to transfect siRNAs into the cells. For the experiments, HAECs were plated on 6-well plates (for Western blotting) or 60-mm culture dishes with a coverslip (for immunofluorescence staining and Western blotting). They were grown in EBM-2 endothelial growth basal medium for 24 h, after which the culture medium was changed to serum-free M199 with Hank's salts. In the meantime, siRNA was incubated with lipofectamine diluted in Opti-MEM medium (Life Technologies/ThermoFisher Scientific) for 15 min at room temperature, which produces siRNA-lipofectamine complexes. Transfection of siRNA was performed by incubating the cells with siRNA-lipofectamine complexes for 6 h at 37 °C in a CO_2 incubator. The cells were then cultured for an additional 18 h in EBM-2 endothelial growth basal medium.

Western blot analysis

Following cell culture treatments, the conditioned medium was either discarded or collected to quantify shedded RAGE. After being cleaned with phosphate-buffered saline (PBS), the residual cells were treated on ice for 10 min with cold RIPA buffer, which included 50 mM Tris-HCl (pH 7.4), 150 mM NaCl, 0.25% sodium deoxycholate, 1% NP-40, and protease and phosphatase inhibitors. The cells that were lysed in RIPA buffer were gathered, transferred to a microcentrifuge tube, and centrifuged at 10,000×*g* for 5 min at 4 °C. The supernatant was obtained as a whole cell lysate. After measuring the protein concentration by the Bradford method, cell lysates with equal protein amounts were separated via sodium dodecyl sulfate-polyacrylamide gel electrophoresis and then transferred to an Immobilon-P membrane (EMD Millipore, Bedford, MA, USA). The primary antibodies were applied to the protein-transferred membranes first, followed by a wash and application of the secondary antibodies conjugated with horseradish peroxidase. Finally, the membranes were washed and incubated with Luminata Forte Western HRP Substrate (EMD Millipore) to see the protein bands.

To quantify shedded RAGE, equal volumes of conditioned medium were concentrated using an Amicon® Ultra centrifugal filter (Ultracel®-10 K, EMD Millipore), and the samples were immunoblotted using an anti-human RAGE antibody (sc-80652), which interacts with the extracellular domain of human RAGE.

Immunofluorescence staining of cell surface ADAM10

In 60-mm culture dishes, a coverslip was placed on the bottom, and the cells were plated and cultured. The cells grown on the coverslip were utilized to stain the cell surface ADAM10 using immunofluorescence. The other cells in the same culture dish underwent Western blot analysis to determine the quantity of ADAM10, AKT1, AKT2, AKT3, or Rab14.

Cells on the coverslip were fixed for 10 min in 4% paraformaldehyde. To detect cell surface ADAM10, permeabilizing agents such as Triton X-100 were not employed. After fixation, cells were treated for 60 min with 1% bovine serum albumin in PBS to block nonspecific binding and then incubated overnight at 4 °C with a rabbit antibody against an extracellular epitope of human ADAM10 (A10438). After three PBS washes, the cells were treated with an AlexaFluor 488-conjugated anti-rabbit IgG secondary antibody. The nuclei of the cells were then

labeled with DAPI. The cells' immunofluorescence images were captured using a Zeiss LSM710 laser-scanning confocal microscope (Carl Zeiss, Oberkochen, Germany). Using the ImageJ software (National Institutes of Health, Bethesda, USA), each cell's fluorescence intensity was calculated as follows: Each cell's fluorescence intensity = integrated density − (the area of the selected cell × the mean fluorescence of background reading).

Co-immunoprecipitation

The cells were lysed with NP-40 Lysis Buffer (MedChemExpress), which contains 50 mM Tris (pH 7.4), 150 mM NaCl, 1% NP-40, and protease inhibitors. At 4 °C, the whole cell lysates (500 μg) were precleared by incubating with 1 μg of rabbit control IgG (Cell Signaling Technology, #2729) and 20 μl of protein A agarose (Santa Cruz Biotechnology, sc-2001) for 30 min and then incubated overnight with 4 μg of a rabbit anti-ADAM10 antibody (MA5-32616) or a rabbit control IgG, followed by incubation with 20 μl of protein A agarose for 4 h. Both the whole cell lysate (input) and the immunoprecipitated proteins were analyzed by Western blot using mouse monoclonal antibodies to ADAM10 (sc-28358) and Rab14 (sc-271401).

Separation of cell surface and intracellular proteins

The Pierce™ cell surface protein biotinylation and isolation kit (ThermoFisher Scientific) was used to separate cell surface proteins from intracellular proteins. Briefly, cells grown in 100-mm culture dishes were treated with either DMSO or SC79. Cell surface proteins were labeled by incubating cells with Sulfo-NHS-SS-Biotin for 10 min at room temperature. To isolate biotin-labeled proteins, NeutrAvidin agarose beads were added to whole cell lysates in spin columns. The proteins that did not adhere to the agarose beads were collected and designated as intracellular proteins. Biotin-labeled proteins adhered to agarose beads were collected using an elution buffer containing dithiothreitol and defined as cell surface proteins. Cell surface proteins, intracellular proteins, and whole cell lysates were subjected to Western blot analysis.

Statistical analysis

Data are presented as mean ± S.E.M. The differences between the two groups were examined using the Student's t test. The differences among the three or more groups were determined using the analysis of variance test with Scheffe's multiple comparisons. IBM SPSS Statistics 21.0. (IBM Co., Armonk, NY, USA) was used to conduct the statistical analyses. *P* values below 0.05 were deemed statistically significant.

Data availability

Data will be available upon request to the corresponding author.

Received: 10 June 2024; Accepted: 14 February 2025
Published online: 03 March 2025

References

1. Dong, H., Zhang, Y., Huang, Y. & Deng, H. Pathophysiology of RAGE in inflammatory diseases. *Front. Immunol.* **13**, 931473 (2022).
2. Hu, P., Lai, D., Lu, P., Gao, J. & He, H. ERK and Akt signaling pathways are involved in advanced glycation end product-induced autophagy in rat vascular smooth muscle cells. *Int. J. Mol. Med.* **29**, 613–618 (2012).
3. Hu, P. et al. Autophagy plays a protective role in advanced glycation end product-induced apoptosis in cardiomyocytes. *Cell. Physiol. Biochem.* **37**, 697–706 (2015).
4. Adachi, N. et al. Insulin-like growth factor-I protects against the detrimental effects of advanced glycation end products and high glucose in myoblastic C2C12 cells. *Calcif Tissue Int.* **105**, 89–96 (2019).
5. Zhao, G., Zhang, X., Wang, H. & Chen, Z. Beta carotene protects H9c2 cardiomyocytes from advanced glycation end product-induced endoplasmic reticulum stress, apoptosis, and autophagy via the PI3K/Akt/mTOR signaling pathway. *Ann. Transl Med.* **8**, 647 (2020).
6. Raucci, A. et al. A soluble form of the receptor for advanced glycation endproducts (RAGE) is produced by proteolytic cleavage of the membrane-bound form by the sheddase a disintegrin and metalloprotease 10 (ADAM10). *FASEB J.* **22**, 3716–3727 (2008).
7. Khezri, M. R., Mohebalizadeh, M. & Ghasemnejad-Berenji, M. Therapeutic potential of ADAM10 modulation in Alzheimer's disease: A review of the current evidence. *Cell. Commun. Signal.* **21**, 60 (2023).
8. Rosenbaum, D. & Saftig, P. New insights into the function and pathophysiology of the ectodomain sheddase a disintegrin and metalloproteinase 10 (ADAM10). *FEBS J.* **291**, 2733–2766 (2024).
9. Baek, C. H., Kim, H., Moon, S. Y., Park, S. K. & Yang, W. S. Epigallocatechin-3-gallate downregulates lipopolysaccharide signaling in human aortic endothelial cells by inducing ectodomain shedding of TLR4. *Eur. J. Pharmacol.* **863**, 172692 (2019).
10. Baek, C. H., Kim, H., Moon, S. Y. & Yang, W. S. Liraglutide, a glucagon-like peptide-1 receptor agonist, induces ADAM10-dependent ectodomain shedding of RAGE via AMPK activation in human aortic endothelial cells. *Life Sci.* **292**, 120331 (2022).
11. Baek, C. H., Kim, H., Moon, S. Y. & Yang, W. S. AMPK boosts ADAM10 shedding activity in human aortic endothelial cells by promoting Rab14-dependent ADAM10 cell surface translocation. *Biochem. Biophys. Res. Commun.* **675**, 54–60 (2023).
12. Homma, Y., Hiragi, S. & Fukuda, M. Rab family of small GTPases: an updated view on their regulation and functions. *FEBS J.* **288**, 36–55 (2021).
13. Mafakheri, S., Chadt, A. & Al-Hasani, H. Regulation of RabGAPs involved in insulin action. *Biochem. Soc. Trans.* **46**, 683–690 (2018).
14. Espelage, L., Al-Hasani, H. & Chadt, A. RabGAPs in skeletal muscle function and exercise. *J. Mol. Endocrinol.* **64**, R1–R19 (2020).
15. Jaldin-Fincati, J. R., Pavarotti, M., Frendo-Cumbo, S., Bilan, P. J. & Klip, A. Update on GLUT4 vesicle traffic: a cornerstone of insulin action. *Trends Endocrinol. Metab.* **28**, 597–611 (2017).
16. Jo, H. et al. Small molecule-induced cytosolic activation of protein kinase Akt rescues ischemia-elicited neuronal death. *Proc. Natl. Acad. Sci. U.S.A.* **109**, 10581–10586 (2012).
17. Gonzalez, E. & McGraw, T. E. Insulin-modulated akt subcellular localization determines akt isoform-specific signaling. *Proc. Natl. Acad. Sci. U S A.* **106**, 7004–7009 (2009).
18. Sharma, M., Dey, C. S., AKT & ISOFORMS-AS160-GLUT4. The defining axis of insulin resistance. *Rev. Endocr. Metab. Disord.* **22**, 973–986 (2021).
19. Sharma, M. & Dey, C. S. Role of akt isoforms in neuronal insulin signaling and resistance. *Cell. Mol. Life Sci.* **78**, 7873–7898 (2021).

20. Zhang, L. et al. Receptor for advanced glycation end products is subjected to protein ectodomain shedding by metalloproteinases. *J. Biol. Chem.* **283**, 35507–35516 (2008).
21. Yang, W. S., Kim, J. J., Lee, M. J., Lee, E. K. & Park, S. K. Ectodomain shedding of RAGE and TLR4 as a negative feedback regulation in high-mobility group box 1-activated aortic endothelial cells. *Cell. Physiol. Biochem.* **51**, 1632–1644 (2018).
22. Suizu, F. et al. The E3 ligase TTC3 facilitates ubiquitination and degradation of phosphorylated akt. *Dev. Cell.* **17**, 800–810 (2009).
23. Stenmark, H. Rab GTPases as coordinators of vesicle traffic. *Nat. Rev. Mol. Cell. Biol.* **10**, 513–525 (2009).
24. Lindsay, A. J. & McCaffrey, M. W. The C2 domains of the class I Rab11 family of interacting proteins target recycling vesicles to the plasma membrane. *J. Cell. Sci.* **117**, 4365–4375 (2004).
25. Erusalimsky, J. D. The use of the soluble receptor for advanced glycation-end products (sRAGE) as a potential biomarker of disease risk and adverse outcomes. *Redox Biol.* **42**, 101958 (2021).
26. Chen, C. D., Podvin, S., Gillespie, E., Leeman, S. E. & Abraham, C. R. Insulin stimulates the cleavage and release of the extracellular domain of Klotho by ADAM10 and ADAM17. *Proc. Natl. Acad. Sci. U.S.A.* **104**, 19796–19801 (2007).
27. Ishikura, S., Bilan, P. J. & Klip, A. Rabs 8A and 14 are targets of the insulin-regulated Rab-GAP AS160 regulating GLUT4 traffic in muscle cells. *Biochem. Biophys. Res. Commun.* **353**, 1074–1079 (2007).
28. Reed, S. E. et al. A role for Rab14 in the endocytic trafficking of GLUT4 in 3T3-L1 adipocytes. *J. Cell. Sci.* **126**, 1931–1941 (2013).
29. Linford, A. et al. Rab14 and its exchange factor FAM116 link endocytic recycling and adherens junction stability in migrating cells. *Dev. Cell.* **22**, 952–966 (2012).
30. Harrison, N., Koo, C. Z. & Tomlinson, M. G. Regulation of ADAM10 by the TspanC8 family of tetraspanins and their therapeutic potential. *Int. J. Mol. Sci.* **22**, 6707 (2021).
31. Shiu, S. W., Wong, Y. & Tan, K. C. Effect of advanced glycation end products on lectin-like oxidized low density lipoprotein receptor-1 expression in endothelial cells. *J. Atheroscler Thromb.* **19**, 1083–1092 (2012).
32. Wang, Y., Ge, X., Yu, S. & Cheng, Q. *Achyranthes bidentata* polypeptide alleviates neurotoxicity of lipopolysaccharide-activated microglia via PI3K/Akt dependent NOX2/ROS pathway. *Ann. Transl Med.* **9**, 1522 (2021).
33. Guo, X. et al. AKT controls NLRP3 inflammasome activation by inducing DDX3X phosphorylation. *FEBS Lett.* **595**, 2447–2462 (2021).
34. Schabbauer, G., Tencati, M., Pedersen, B., Pawlinski, R. & Mackman, N. PI3K-Akt pathway suppresses coagulation and inflammation in endotoxemic mice. *Arterioscler. Thromb. Vasc Biol.* **24**, 1963–1969 (2004).
35. Jing, Z. T. et al. AKT activator SC79 protects hepatocytes from TNF-α-mediated apoptosis and alleviates d-Gal/LPS-induced liver injury. *Am. J. Physiol. Gastrointest. Liver Physiol.* **316**, G387–G396 (2019).

Acknowledgements
This study was supported by a grant (2023IL0012) from the Asan Institute for Life Sciences, Asan Medical Center, Seoul, Korea.

Author contributions
C.H.B. and H.K. performed the experiments and prepared the first draft of the manuscript. S.Y.M. performed the experiments. E.K.L. analyzed the data and prepared figures. W.S.Y. designed and supervised the work and edited the manuscript. All authors reviewed the manuscript.

Declarations

Competing interests
The authors declare no competing interests.

Additional information
Supplementary Information The online version contains supplementary material available at https://doi.org/10.1038/s41598-025-90624-w.

Correspondence and requests for materials should be addressed to W.S.Y.

Reprints and permissions information is available at www.nature.com/reprints.

Publisher's note Springer Nature remains neutral with regard to jurisdictional claims in published maps and institutional affiliations.

Open Access This article is licensed under a Creative Commons Attribution-NonCommercial-NoDerivatives 4.0 International License, which permits any non-commercial use, sharing, distribution and reproduction in any medium or format, as long as you give appropriate credit to the original author(s) and the source, provide a link to the Creative Commons licence, and indicate if you modified the licensed material. You do not have permission under this licence to share adapted material derived from this article or parts of it. The images or other third party material in this article are included in the article's Creative Commons licence, unless indicated otherwise in a credit line to the material. If material is not included in the article's Creative Commons licence and your intended use is not permitted by statutory regulation or exceeds the permitted use, you will need to obtain permission directly from the copyright holder. To view a copy of this licence, visit http://creativecommons.org/licenses/by-nc-nd/4.0/.

© The Author(s) 2025